

## Connectivity based segmentation of the periaqueductal grey matter in humans with diffusion tensor imaging

Martyn Ezra<sup>1</sup>, Olivia Kate Faull<sup>1</sup>, Saad Jbabdi<sup>2</sup>, and Kyle Thomas Shane Pattinson<sup>1</sup>

<sup>1</sup>Nuffield Department of Clinical Neuroscience, University of Oxford, Oxford, Oxfordshire, United Kingdom, <sup>2</sup>Oxford Centre for Functional Magnetic Resonance Imaging of the Brain, University of Oxford, Oxford, Oxfordshire, United Kingdom

### Introduction

The midbrain periaqueductal gray matter (PAG) is involved in a number of key homeostatic neurobiological functions, such as pain modulation and cardiorespiratory control. Currently, most of our understanding of its structure and function comes from animal research, and the translation of these findings to humans has yet to be accomplished non-invasively. Despite its cytoarchitectonic (and MRI) homogeneity, animal models have shown significant heterogeneity with respect to functional properties, anatomical connections and chemical properties between subdivisions of the PAG<sup>1</sup>. These subdivisions are proposed as four longitudinal columns parallel to the aqueduct, and their identification *in vivo* is critical to improving our understanding of the PAG and its use in interventional therapies such as deep brain stimulation (DBS). Previous attempts to segment the human PAG have yielded disappointing results<sup>2</sup>, in part due to its small size and location. This study used high resolution diffusion tensor imaging (DTI) to segment the PAG based upon voxel connectivity profiles.

### Materials and methods

Nineteen right handed healthy subjects were included in this study (6 women and 13 men; range, 23–40 years). Diffusion weighted images were acquired on a Siemens Trio 3T scanner with a 12-channel head coil using an echo planar imaging sequence (3 acquisitions of 60 directions with 5 non-diffusion weighted images, b-value 1000 s mm<sup>-2</sup>, voxel size 1.5×1.5×1.5 mm, 100 slices, cardiac gated). Probabilistic diffusion tractography between the PAG and whole brain was carried out using the FSL toolbox<sup>3</sup>. A cross-correlation matrix between the connectivity profiles of all voxels in the PAG mask was segmented using a k means clustering algorithm. K means clustering requires the number of clusters to be selected a priori, 4 clusters were chosen to match the animal model of the PAG. A group probability map for each cluster was produced in MNI standard space to display the final results. Individual subject clusters that demonstrated satisfactory segmentation then underwent thresholding to remove voxels with a silhouette value <0.25 to exclude voxels that overlapped columns. These clusters were used as seeds to generate connectivity profiles with predefined target regions known to have PAG connectivity and as targets for whole brain back projection.

### Results

Clustering was able to segment the PAG into four distinct clusters that demonstrated good spatial concordance with the columns derived from animal model of the PAG (Fig 1a and 1b). We suggest that Cluster 1 is the dorsomedial PAG, Cluster 2 the dorsolateral PAG, Cluster 3 the lateral PAG and Cluster 4 the ventrolateral PAG. The relative connectivity of the clusters to 12 target regions revealed distinct connectivity profiles for each cluster (Fig 2). These results show that the human PAG has a structure similar to that identified in non human studies, however the connectivity patterns of these subdivisions are markedly different. Most notable is that the ventrolateral PAG demonstrates dominant connectivity to the prefrontal cortical structures in humans whereas in animal studies it is derived from the dorsolateral and lateral PAG<sup>1</sup>. In addition the dorsolateral PAG demonstrates connectivity to the medulla, which is absent in animal studies. Whole brain back projections identified differential spatial connectivity within the medulla to the PAG, with the ventrolateral and dorsolateral PAG demonstrating preferential connectivity to dorsomedial medulla, and ventrolateral medulla respectively (Fig 1c).

Fig 1.

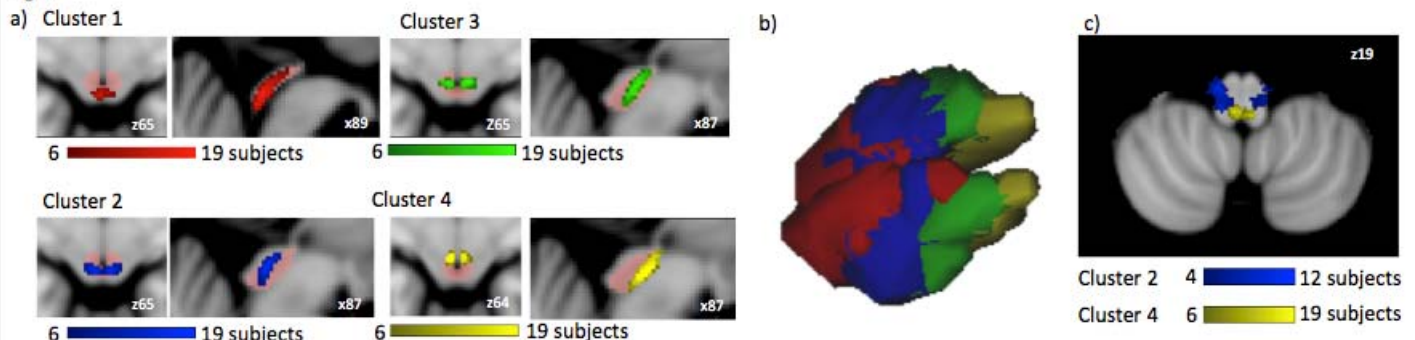


Fig 1. a) Group probability maps of clustering results over PAG mask (Pink). Axial and right sided sagittal (left side omitted as equivalent to right) slices taken at the average MNI coordinate for the centre of gravity of the cluster(s). b) 3D rendering of the PAG with hard segmentation of clustering results. c) Axial slice through the medulla (MNI coordinate top right) with group probability maps of the whole brain back projections.

### Discussion

This is the first study that has been able to resolve distinct subdivisions within the human PAG. High resolution DTI and cardiac gated acquisitions (used to minimize artefacts from pulsatile flow of the cerebrospinal fluid) have enabled the segmentation of the PAG, despite its small size and location. The resolution of the subdivisions for individual subjects has permitted detailed examination of their structural connectivity without the a priori selection of a starting location based on an assumed spatial location<sup>4</sup>. This has resulted in the identification of differences in structural connectivity of the PAG between animals and humans. These findings are of critical importance in understanding the function of the PAG in humans. The different division of the PAG are known to different functions, such as cardiovascular control<sup>4</sup> and analgesia. The ability to resolve the subdivision *in vivo* may aid in planning and improving stereotactic interventions such as DBS and in the interpretation of functional imaging studies particularly as high field strength fMRI becomes able to resolve activation within these subdivisions.

### References

1. Bandler et al. Brain Research Bulletin. 2000, 53(1), 95–104. PMID 11033213
2. Linnman et al. NeuroImage. 2012, 60(1), 505–22. PMID 22197740
3. Johansen-Berg et al. PNAS. 2004, 101(36), 13335–40. PMID 15340158
4. Pereira et al. Experimental Neurology. 2010, 223(2), 574–81. PMID 20178783

Fig 2.

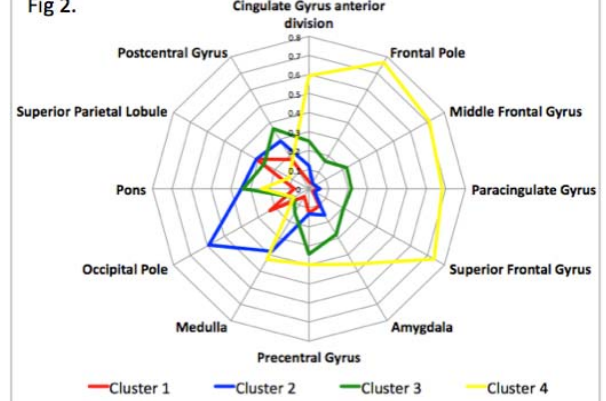


Fig 2. Radial diagram of relative connectivity of the clusters to predefined targets.